Article

Not peer-reviewed version

# Identify Novel Targeting Sites of Calcineurin and CaMKII in Human Cav3.2 T-type Calcium Channel

Yu-Wang Chang [*] , Yong-Cyuan Chen , Chien-Chang Chen [*]

Posted Date: 16 August 2023

doi: 10.20944/preprints202308.1114.v1

Keywords: Phosphorylation; dephosphorylation; CaV3.2 T-type calcium channel; calcineurin; CaMKII

*Article*

# Identify Novel Targeting Sites of Calcineurin and CaMKII in Human Cav3.2 T-type Calcium Channel

**Yu-Wang Chang *, Yong-Cyuan Chen and Chien-Chang Chen ***

Institute of Biomedical Sciences, Academia Sinica, Taipei 11529, Taiwan; joyoyo@ibms.sinica.edu.tw (Y.-C.C.); awanya@ibms.sinica.edu.tw (Y.-W.C.)

* Correspondence: awanya@ibms.sinica.edu.tw (Y.-W.C.); ccchen@ibms.sinica.edu.tw (C.-C.C.);

**Abstract:** The Cav3.2 T-type calcium channel is implicated in various pathological conditions, including cardiac hypertrophy, epilepsy, autism, and chronic pain. Phosphorylation of Cav3.2 by multiple kinases plays a pivotal role in regulating its calcium channel function. The calcium/calmodulin-dependent serine/threonine phosphatase, calcineurin, interacts physically with Cav3.2 and modulates its activity. However, it remains unclear whether calcineurin dephosphorylates Cav3.2, the specific spatial regions on Cav3.2 involved, and the extent of the quantitative impact. In this study, we elucidated the serine/threonine residues on Cav3.2 targeted by calcineurin using quantitative mass spectrometry. We identified six serine residues in the N-terminus, II-III loop, and C-terminus of Cav3.2 that were dephosphorylated by calcineurin. Notably, a higher level of dephosphorylation was observed in the Cav3.2 C-terminus, where calcineurin binds to this channel. Additionally, a previously known CaMKII-phosphorylated site, S1198, was found to be dephosphorylated by calcineurin. Furthermore, we also discovered that a novel CaMKII-phosphorylated site, S2137, underwent dephosphorylation by calcineurin. In CAD cells, a mouse central nervous system cell line, membrane depolarization led to an increase in the phosphorylation of endogenous Cav3.2 at S2137. Mutation of S2137 affected the calcium channel function of Cav3.2. Our findings advance the understanding of Cav3.2 regulation not only through kinase phosphorylation but also via calcineurin phosphatase dephosphorylation.

**Keywords:** phosphorylation; dephosphorylation; Cav3.2 T-type calcium channel; calcineurin; CaMKII;

## 1. Introduction

Calcium entry through voltage-gated calcium channels depolarizes the membrane potential, facilitating the transmission of electrical signals in nerve and muscle tissues [1]. Additionally, intracellular calcium serves as a crucial secondary messenger, governing diverse cell signaling pathways and biological processes [2]. The regulation of intracellular calcium concentration involves both high-voltage-activated calcium channels (Cav1 and Cav2 subtypes) and low-voltage-activated calcium channels (Cav3 subtypes). The low-voltage-activated calcium channels, known as T-type (T for transient or tiny) channels, exhibit rapid inactivation kinetics and are capable of opening near the resting membrane potential, contributing to membrane depolarization. Vertebrates express three different T-type calcium channels: Cav3.1, Cav3.2, and Cav3.3 [3,4]. Dysfunctions in T-type calcium channels are linked to various disease conditions, including epilepsy, autism, neuromuscular disorders, and chronic pain [5]. Cav3.2 exhibits high expression levels in dorsal root ganglion sensory neurons and plays an important role in the development of chronic pain [6,7].

The pore-forming $\alpha$1-subunit of T-type calcium channels consists of four homologous transmembrane domains connected by cytoplasmic N-terminus, interdomain loops, and C-terminus. These cytoplasmic regions of T-type calcium channels serve as sites of posttranslational modifications by intracellular enzymes, thereby fine-tuning the channel functions [8,9]. Deubiquitination of Cav3.2 by USP5 promotes channel stability and function, thus mediating the development of neuropathic and inflammatory pain in rodents [7]. Additionally, various kinases modulate the functions of Cav3.2 through phosphorylation. Phosphorylation of Cav3.2 at the S1107 residue in the II-III loop by PKA is required for G$\beta\gamma$-mediated inhibition of Cav3.2 [10]. Phosphorylation of Cav3.2 at the S1198 residue

 doi:10.20944/preprints202308.1114.v1



in the II-III loop by CaMKII causes a leftward shift in the activation threshold and facilitates channel opening near the resting membrane potential [11,12]. Moreover, phosphorylation of Cav3.2 at S561 in the I-II loop and S1987 in the C-terminus by Cdk5 upregulates channel current density [13]. Although activation of kinases, including ROCK and PKC, facilitates the Cav3.2 current, the detailed phosphorylation sites at Cav3.2 remain unclear [14,15].

The activity of Cav3.2 is further influenced by specific proteins that interact with its cytoplasmic regions. Syntaxin-1A, for instance, binds to the C-terminus of Cav3.2 channels, regulating both channel function and low-threshold exocytosis [16]. Additionally, calcineurin also binds to the C-terminus of Cav3.2 channels, resulting in a reduction of channel current density [17]. This interaction between Cav3.2 and calcineurin is dependent on calmodulin and calcium concentration. The NFAT-binding domain of calcineurin is essential for its binding to Cav3.2. Moreover, the PCISVE (2190-2195) and LTVP (2261-2264) motifs in the C-terminus of Cav3.2 are crucial for the channels' interaction with calcineurin. The 9A-Cav3.2 mutant form, which cannot bind to calcineurin, also exhibits a higher current density [17].

Calcineurin is a serine/threonine phosphatase known for dephosphorylating various target proteins, including transcription factors, receptors, and channels [18]. Notably, the dephosphorylation of the transcription factor NF-AT3 by calcineurin is implicated in pathological cardiac hypertrophy [19,20]. Similarly, Cav3.2 is also involved in the development of pathological cardiac hypertrophy [21]. While it is established that calcineurin interacts with and modulates Cav3.2, the specific dephosphorylation of Cav3.2 by calcineurin has remained unclear. In this study, we aimed to identify the serine/threonine residues of Cav3.2 channels targeted by calcineurin for dephosphorylation. Additionally, we discovered that the CaMKII phosphorylates one of the calcineurin-targeted residues, namely S2137. Interestingly, we observed that membrane depolarization increased the S2137 phosphorylation, as confirmed by its specific antibody. The functional implications of S2137 phosphorylation were also investigated in this study.

## 2. Materials and methods

### *2.1. Plasmid cDNA Construction and Mutagenesis*

The generation of mutant plasmid constructs was accomplished using the QuikChange site-directed mutagenesis kit (Agilent Technologies, Santa Clara, CA, USA). Following mutagenesis, the integrity of the constructs was confirmed through sequencing. The C-terminus of human Cav3.2 were amplified by PCR and cloned into pGEX-4T-1 (Thermo Fisher Scientific, Waltham, MA, USA).

### *2.2. Cell Culture and Transient Expression*

Human embryonic kidney (HEK) 293 cells and mouse catecholaminergic neuronal CAD cells were cultivated in Dulbecco's modified Eagle's medium (DMEM), supplemented with 5% fetal bovine serum and penicillin/streptomycin, at 37°C in a 5% CO2 incubator. For transient transfection, HEK293 cells were transfected with 5 μg of plasmid DNA using the calcium-phosphate method. Plasmids encoding Flag-tagged Cav3.2, 9A-Cav3.2, S1198A-Cav3.2, S2137A-Cav3.2, S2137D-Cav3.2, S1198A-9A-Cav3.2, S2137A-9A-Cav3.2, and S1198AS2137A-9A-Cav3.2 were individually transfected into HEK-293 cells. The GST-fusion C-terminus of Cav3.2 (GST-CII) was transfected into HEK-293 cells. Following transfection, cells were incubated at 37°C for 48 hours before being subjected to cell lysis, immunoprecipitation, and whole-cell voltage-clamp recordings. To administer cyclosporine A (CSA), the cells were subjected to a 24-hour incubation with CSA following 1 day of transfection.

### *2.3. Cell Lysis and Immunoprecipitation*

Transfected cells were lysed and homogenized using an immunoprecipitation buffer composed of the following components: (in mM) 50 Tris HCl, pH 8.0, 150 sodium chloride, 1% Triton-X100, 1 mM EDTA, protease inhibitors, and phosphatase inhibitors. The resulting lysates were incubated on ice for 30 minutes. Subsequently, undissolved pellets were separated by centrifugation at 13,000 rpm for 30 minutes at a temperature of 4 °C. For immunoprecipitation, the cell lysates were subjected to

 doi:10.20944/preprints202308.1114.v1



incubation with anti-FLAG antibody-conjugated beads (Sigma–Aldrich, Saint Louis, MO, USA) at 4°C overnight, utilizing rotation. For the *in vitro* calcineurin reaction, the pulled-down Flag-Cav3.2 was washed successively with lysis buffer, PBS, and calcineurin reaction buffer. The Flag-Cav3.2 was eluted by the 3xFlag peptide (Sigma–Aldrich). For the GST-pull down procedure, the GST-fusion protein consisting of the C-terminus of Cav3.2 (GST-CII) was extracted using glutathione sepharose beads (GE Healthcare, Chicago, IL, USA). Following a thorough wash, the proteins that bound to the beads were eluted by employing an excess amount of reduced glutathione [17].

### *2.4. In Vitro Calcineurin and CaMKII reactions*

In the context of the in vitro calcineurin reaction, the pulled-down Flag-Cav3.2 was subjected to incubation with active calcineurin enzyme, human recombinant calmodulin, and calcineurin reaction buffer (Abcam, Cambridge, UK). For the control sample, incubation was performed without the active calcineurin enzyme. Following a 1-hour incubation at 37°C, the Flag-Cav3.2 samples were either prepared for gel-assisted digestion or immunoblotting. For the CaMKII reaction, the C-terminus of Cav3.2 (GST-CII) or Flag-Cav3.2 were incubated with CaMKII, calmodulin, and NEB buffer for protein kinases (New England Biolabs, Ipswich, MA, USA). After a 1-hour incubation at 37°C, the GST-CII samples were subjected to SDS-PAGE and stained with Coomassie blue. The resulting gel bands were excised for in-gel digestion. The CaMKII-treated Falg-Cav3.2 was prepared for immunoblotting.

### *2.5. Gel-Assisted Digestion, In-Gel Digestion, and Immobilized Metal Affinity Chromatography*

Gel-assisted digestion was employed to enhance the efficiency of digesting membrane proteins [22]. To assess variations in digestion efficiency, 0.2 µg of bovine α-casein and 0.05 µg bovine β-casein were added into eluted Flag-Cav3.2 samples. Proteins were reduced using 5 mM tris(2-carboxyethyl)phosphine, followed by alkylation with 2 mM MMTS at room temperature for 30 minutes. For direct incorporation of proteins into a gel within a micro tube, acrylamide/bisacrylamide solution, APS, and TEMED were added to the protein solution. The gel was fragmented into small pieces and subjected to multiple washes with 0.5 ml of TEABC containing 50% (v/v) ACN. Subsequently, the gel samples were dehydrated using 100% ACN and thoroughly dried using a vacuum centrifuge. Next, proteolytic digestion was carried out with trypsin in 25 mm TEABC with overnight incubation at 37 °C. Peptides were extracted from the gel using a sequential extraction process involving 200 µl of 25 mM TEABC, 200 µl of 0.1% (v/v) TFA in water, 200 µl of 0.1% (v/v) TFA in ACN, and 200 µl of 100% ACN. The extracted solutions were combined and concentrated using a vacuum centrifuge. For in-gel digestion of GST-CII, the gel bands were fragmented into small pieces, washed with 0.5 ml of TEABC containing 50% (v/v) ACN, completely dried by 100% ACN and vacuum centrifuge, followed by trypsin digestion. The resulting peptides were then extracted. Phosphopeptide enrichment using immobilized metal affinity chromatography (IMAC) was carried out following previously reported procedures [23]. The IMAC eluate and tryptic peptides were subsequently purified using a C18 Ziptip (Millipore, Bedford, MA, USA) for cleaning.

### *2.6. Mass Spectrometry (MS), Database Searching and Phosphopeptide Quantification*

The phosphopeptides enriched through IMAC and the tryptic peptides of different variants of Cav-3.2 were subjected to analysis using reverse-phase ultra-performance liquid chromatography (nanoACQUITY UPLC, Waters, Milford, MA, USA) in conjunction with quadruple time-of-flight MS (QTOF Premier, Waters), following the established procedure [23]. The MS peak lists were generated in Mascot generic format (mgf) using Mascot Distiller with default parameters. The mgf files were employed for searching against the UniProt human protein database using Mascot (Matrix Science, London, UK). The database searching parameters included trypsin as the protease, allowance for up to 2 missed cleavages, and tolerances of 0.07 Da for both precursor and fragment ion measurements. Variable modifications were set to include methylthio of cysteine, oxidation of methionine, and phosphorylation of serine, threonine, and tyrosine. Proteins were considered identified if they met

 doi:10.20944/preprints202308.1114.v1



the significance threshold of $p < 0.05$. Peptides were considered identified if they had a peptide score of 30 or higher. The Mascot delta score was utilized for phosphorylation site assignment [23,24]. Peptide and phosphopeptide quantification was achieved using IDEAL-Q [25]. Bovine $\alpha$-casein and $\beta$-casein, added externally, served as internal references for the quantification of Cav3.2 phosphopeptides. To achieve this, each mgf file was subjected to a Mascot search against the UniProt bovine protein database. The quantities of bovine casein peptides or phosphopeptides were determined using IDEAL-Q and employed for the normalization of peptides or phosphopeptides of Cav3.2.

### *2.7. Generation of Phospho-S2137 Cav3.2 Antibody and Immunoblotting*

The preparation of the rabbit polyclonal phospho-S2137 Cav3.2 antibody included the synthesis of a corresponding peptide with phosphoserine at the indicated site. This synthetic peptide was then conjugated to BSA before being used as the peptide antigen for immunizing the host rabbits. For immunoblotting, the pulled-down GST-CII or Flag-Cav3.2, the cell lysates of transfected HEK293 cells, and the cell lysates of CAD cells were separated using SDS-PAGE. Subsequently, they were transferred onto a PVDF membrane for immunostaining using specific antibodies. The following antibodies were utilized: anti-Cav3.2 (H-300, Santa Cruz Biotechnologies, Inc.), anti-Flag (M2-HRP, Sigma-Aldrich), anti-$\beta$ actin (Proteintech, Chicago, IL, USA), and a homemade anti-phospho-S2137 Cav3.2 antibody.

### *2.8. Electrophysiological Recording*

Patch pipettes with a tip resistance ranging from 2.8 to 3.5 MΩ were fashioned from borosilicate glass capillary tubes (Warner Instruments, Holliston, MA, USA) utilizing a P-97 Flaming-Brown type micropipette puller (Sutter Instrument, Novato, CA, USA). Ionic currents were recorded using an Axon Multiclamp 700B microelectrode amplifier (Molecular Devices, San Jose, CA, USA). Data acquisition occurred at a sampling frequency of 50 kHz, with a low-pass filter set at 2 kHz. Control of voltage and current commands, as well as the digitization of membrane voltages and currents, were achieved through a Digidata 1440A interfaced with Clampex 10.4 (Molecular Devices, San Jose, CA, USA). The analysis of data was conducted using pCLAMP10.4 software (Molecular Devices, San Jose, CA, USA). To measure Cav3.2 currents, cells were bathed in a solution consisting of the following constituents (in mM): 145 TEA-Cl, 5 CaCl2, 3 CsCl, 1 MgCl2, 5 glucose, and 10 HEPES, adjusted to a pH of 7.4 using TEA-OH, with an osmolarity of approximately 300 mOsm. The composition of the pipette solution was as follows (in mM): 130 CsCl, 20 HEPES, 10 EGTA, 5 MgCl2, 3 Mg-ATP, and 0.3 Tris-GTP, adjusted to a pH of 7.3 using CsOH, with an osmolarity of approximately 310 mOsm. All recordings were conducted at room temperature (21–24 °C). For cells transfected with Cav3.2, their membrane potentials were initially maintained at −90 mV for 20 ms and subsequently depolarized to −30 mV for 150 ms. The reduction in peak amplitudes induced by toxins indicated changes in peak values before and after toxin addition. The degree of inhibition was calculated by dividing the toxin-reduced peak amplitudes by the peak amplitudes before toxin addition.

## 3. Results

### *3.1. Identification of Amino Acid Residues on Cav3.2 Dephosphorylated by Calcineurin*

Calcineurin, a calcium/calmodulin-dependent protein phosphatase, interacts with and modulates the functions of Cav3.2 T-type calcium channels [17]. To investigate whether calcineurin regulates Cav3.2 through dephosphorylation of specific serine or threonine residues, we expressed Flag-tagged human Cav3.2 in HEK293 cells. For the identification of the exact amino acid residues of Cav3.2 dephosphorylated by calcineurin, we performed mass spectrometry-based identification and label-free quantification of IMAC-enriched phosphopeptides (Supplementary Figure S1). Flag-tagged Cav3.2 was immunoprecipitated (IP) using an anti-Flag antibody and subsequently eluted with 3xFlag peptide. The pulled-down Cav3.2 channels were then reacted with or without calcineurin

Preprints (www.preprints.org) | NOT PEER-REVIEWED | Posted: 16 August 2023 doi:10.20944/preprints202308.1114.v1



and digested into tryptic peptides using gel-assisted digestion [22]. The phosphopeptides were enriched through immobilized metal affinity chromatography (IMAC). The identities and quantities of peptides or phosphopeptides were revealed by LC-MS/MS analysis and IDEAL-Q software [25]. To account for quantification bias resulting from different digestion and purification efficiencies, we incorporated the standard phosphoproteins bovine $\alpha$- and $\beta$-casein as spike-in controls [23]. In total, we identified 39 phosphopeptides matching Cav3.2 (Supplementary Figure S2). Among these phosphopeptides, 30 had single phosphorylation sites, 7 had double phosphorylation sites and 2 had more than three phosphorylation sites (Table 1).

The assignment of phosphorylation sites in a peptide was based on the Mascot delta score of each MSMS spectrum [24]. For example, the MSMS spectrum of a doubly charged phosphopeptide with mass to charge ratio (m/z) of 873.41 corresponded to the amino acid residues from 2135 to 2149 of human Cav3.2. The phosphorylation site was determined as S2137, relying on the Mascot delta score difference between the first and second hits of potential candidate sequences (Figure 1A and Table 1). In this study, 36 phosphosites were assigned, with 34 phosphoserine and 2 phosphothreonine residues. These phosphosites were distributed as follows: 5 in the N-terminus, 9 in the I-II loop, 11 in the II-III loop, 4 in the III-IV loop, and 7 in the C-terminus of Cav3.2 (Figure 1B). Comparing our findings with the results of Blesneac et al. [26] and the PhosphoSitePlus database [27], we identified 8 novel phosphorylation sites at S44, S719, S722, S1109, S1165, S1168, S1604, and S2030.

**Table 1.** Human Cav3.2 phosphorylation sites identified from indicated mass spectra.

| spectra_No.[a] | exp_mz[b] | phosphopeptide_matched[c] | start[d] | end[d] | site[e] | delta_score[g] | score[f] |
|---|---|---|---|---|---|---|---|
| 1 | 800.40 | VPLGAPPPGPAALVGASPE*pS*PGAPG R | 13 | 38 | S32 | 70 | 20 |
| 2 | 827.07 | VPLGAPPPGPAALVGA*pS*PE*pS*PGAP GR | 13 | 38 | S29, S32 | 48 | 39 |
| 3 | 1069.48 | EAERG*pS*ELGVSPSESPAAER | 39 | 58 | S44 | 133 | 50 |
| 4 | 826.87 | GSELGV*pS*PSESPAAER | 43 | 58 | S49 | 86 | 19 |
| 5 | 866.85 | GSELGV*pS*PSE*pS*PAAER | 43 | 58 | S49, S53 | 75 | 11 |
| 6 | 766.64 | EAERG*pS*ELGV*pS*PSE*pS*PAAER | 39 | 58 | S44, S49, S53 | 36 | 6 |
| 7 | 1327.08 | HL*pS*NDSTLASFSEPGSCYEELLK | 440 | 462 | S442 | 84 | 7 |
| 8 | 585.77 | AGAPP*pS*PPSPGR | 553 | 564 | S558 | 37 | 16 |
| 9 | 585.77 | AGAPPSPP*pS*PGR | 553 | 564 | S561 | 31 | 21 |
| 10 | 625.75 | AGAPP*pS*PP*pS*PGR | 553 | 564 | S558, S561 | 35 | 26 |
| 11 | 824.38 | WAGGPPGTGGHGPLSLN*pS*PDPYEK | 636 | 659 | S653 | 40 | 8 |
| 12 | 1043.92 | ALEDPEGEL*pS*GSESGDSDGR | 706 | 725 | S715 | 128 | 29 |
| 13 | 1083.90 | ALEDPEGEL*pS*G*pS*ESGDSDGR | 706 | 725 | S715, S717 | 93 | 25 |
| 14 | 1177.44 | ALEDPEGELpSGpSEpSGDpSDGRGV YEFTQDVR | 706 | 735 | S715, S717, S719, S722 | 54 | 10 |
| 15 | 709.30 | ATDTPGPGPG*pS*PQR | 748 | 761 | S758 | 47 | 24 |
| 16 | 1123.46 | SDTDEDKT*pS*VHFEEDFHK | 1027 | 1044 | S1035 | 69 | 7 |
| 17 | 820.38 | SSPFLDAAP*pS*LPDSR | 1090 | 1104 | S1099 | 74 | 14 |
| 18 | 860.37 | SSPFLDAAP*pS*LPD*pS*R | 1090 | 1104 | S1099, S1103 | 36 | 13 |
| 19 | 898.43 | SSPFLDAAPSLPD*pS*RR | 1090 | 1105 | S1103 | 41 | 21 |
| 20 | 730.35 | RG*pS*SSSGDPPLGDQKPPASLR | 1105 | 1125 | S1107 | 77 | 6 |
| 21 | 1135.00 | RG*pS*S*pS*SGDPPLGDQKPPASLR | 1105 | 1125 | S1107, S1109 | 43 | 6 |
| 22 | 558.26 | S*pS*WSSLGR | 1143 | 1150 | S1144 | 43 | 10 |
| 23 | 711.29 | E*pS*LLSGEGKGSTDDEAEDGR | 1164 | 1183 | S1165 | 49 | 7 |
| 24 | 500.23 | ESLL*pS*GEGK | 1164 | 1172 | S1168 | 55 | 30 |
| 25 | 711.29 | ESLLSGEGKG*pS*TDDEAEDGR | 1164 | 1183 | S1174 | 75 | 6 |
| 26 | 616.21 | GS*pT*DDEAEDGR | 1173 | 1183 | T1175 | 36 | 9 |

Preprints (www.preprints.org) | NOT PEER-REVIEWED | Posted: 16 August 2023 doi:10.20944/preprints202308.1114.v1



| | | | | | | | |
|---|---|---|---|---|---|---|---|
| 27 | 1106.43 | ESLLSGEGKG***pS******pT***DDEAEDGR | 1164 | 1183 | S1174, T1175 | 113 | 35 |
| 28 | 670.35 | AE***pS***LDPRPLRPAALPPTK | 1196 | 1213 | S1198 | 30 | 23 |
| 29 | 504.58 | RR***pS***TFPSPEAQR | 1585 | 1596 | S1587 | 47 | 12 |
| 30 | 531.23 | RR***pS******pT***FPSPEAQR | 1585 | 1596 | S1587, T1588 | 32 | 8 |
| 31 | 600.26 | STFP***pS***PEAQR | 1587 | 1596 | S1591 | 34 | 18 |
| 32 | 542.25 | RPYYADY***pS***PTRR | 1597 | 1608 | S1604 | 46 | 11 |
| 33 | 892.92 | VDADRPPLPQE***pS***PGAR | 1894 | 1909 | S1905 | 50 | 31 |
| 34 | 622.30 | SGEPLHAL***pS***PR | 1991 | 2001 | S1999 | 62 | 38 |
| 35 | 910.42 | ID***pS***PRDTLDPAEPGEK | 2028 | 2043 | S2030 | 55 | 22 |
| 36 | 619.65 | TPVRPVTQGGSLQ***pS***PPR | 2044 | 2060 | S2057 | 91 | 36 |
| 37 | 873.42 | LY***pS***VDAQGFLDKPGR | 2135 | 2149 | S2137 | 92 | 33 |
| 38 | 839.13 | KM***pS***PPCISVEPPAEDEGSARPSAAE GGSTTLR | 2186 | 2217 | S2188 | 42 | 12 |
| 39 | 460.86 | RTP***pS***CEATPHR | 2219 | 2229 | S2222 | 46 | 14 |

[a] The MSMS spectrum is designated as Supplementary Figure S2.; [b] Exp_mz: observed m/z ratio; [c] Phosphorylation sites are indicated with "*p*" before the abbreviation of serine (S) or threonine (T).; [d] Amino acid positions denoting the beginning and end of phosphopeptides in human Cav3.2.; [e] Amino acid positions indicating the sites of phosphorylation.; [f] The Mascot score of the identified phosphopeptide. [g] The Mascot delta score of the specified MSMS spectrum.

To identify the amino acid residues dephosphorylated by calcineurin, we compared the ion signal intensities of phosphopeptides from Cav3.2 channels treated with or without calcineurin. In Figure 1C, the selective ion chromatograms (XICs) of indicated m/z ratios matched to phosphopeptides with single phosphorylation sites were considered candidates with higher priority. We observed a decrease in ion intensities for 5 single-phosphorylated peptides upon treatment with calcineurin. Specifically, S1999, S2137, and S2222 were located in the C-terminus of Cav3.2, while S1144 and S1198 were in the II-III loop. Therefore, we suggest that calcineurin dephosphorylates Cav3.2 at S1144, S1198, S1999, S2137, and S2222.

Interestingly, the ion intensity of the S2188 single-phosphorylated peptide increased upon incubation with calcineurin. It should be noted that S2188 is located close to the calcineurin-binding motif PCISVE (amino acid 2190-2195) of Cav3.2 [17]. One possibility is that the binding of calcineurin may stabilize the phosphorylation at S2188. Another possibility is that a di-phosphorylated peptide might have undergone dephosphorylation in one residue, leading to an increased level of single-phosphorylated peptide phosphorylated in another residues. However, we did not find the corresponding di-phosphorylated peptide of S2188. Conversely, we found an S29S32 di-phosphorylated peptide whose signal intensity was decreased by calcineurin, while the corresponding S32 single-phosphorylated peptide showed an increase (Figure 1D). These results suggest calcineurin dephosphorylates Cav3.2 at N-terminus S29.

Preprints (www.preprints.org) | NOT PEER-REVIEWED | Posted: 16 August 2023 doi:10.20944/preprints202308.1114.v1



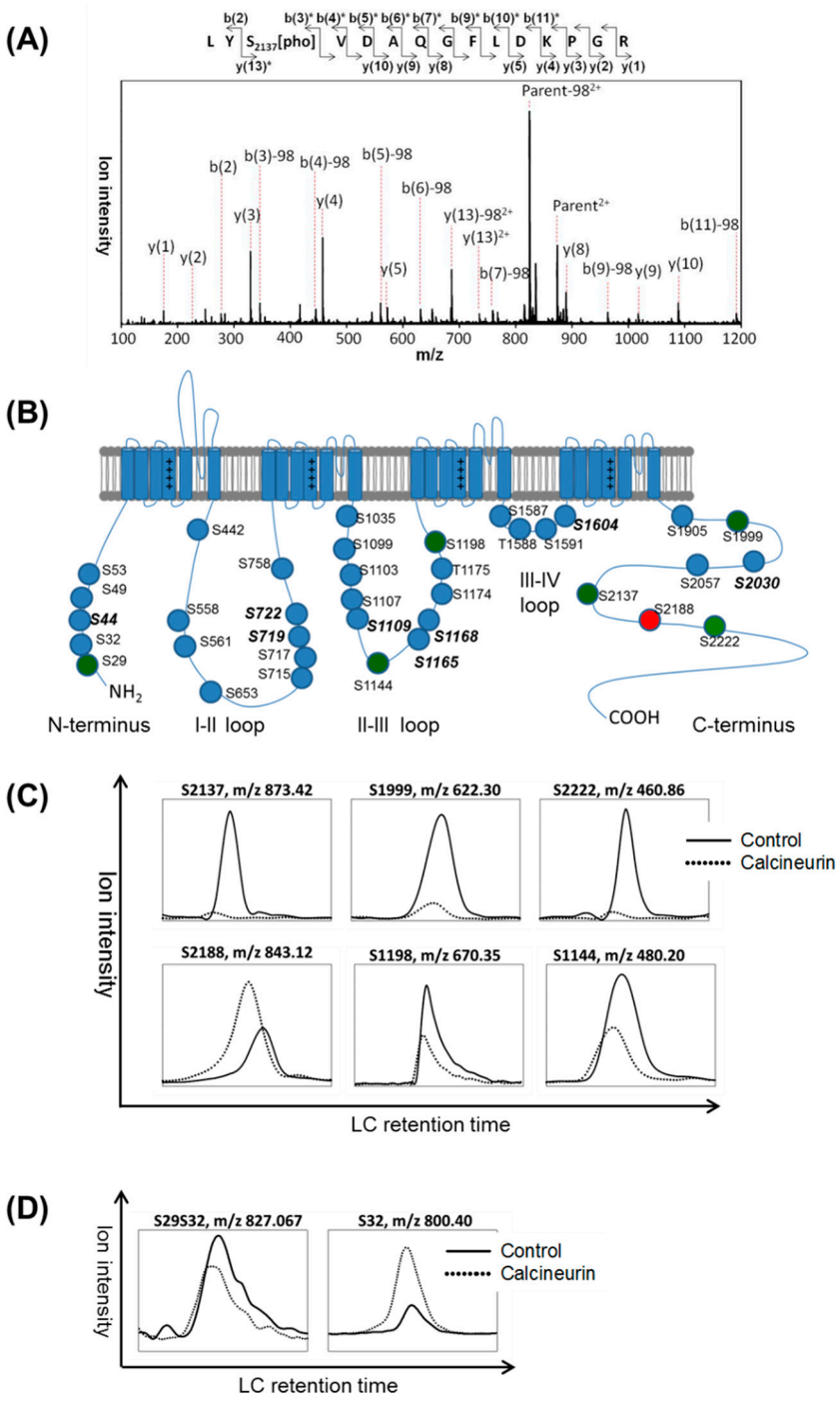


**Figure 1.** Amino acid residues on human Cav3.2 dephosphorylated by calcineurin *in vitro*. (A) MSMS spectrum of a doubly charged ion with m/z 873.41 matched a phosphopeptide belonging to human Cav3.2, spanning residues 2135 to 2149, with phosphorylation on S2137. (B) Cav3.2 phosphorylation sites identified in this study. Phosphorylation of residues highlighted in green indicates a decrease, while phosphorylation of residues highlighted in red indicates an increase in response to calcineurin treatment. Phosphorylation sites emphasized in bold italic font are previously unidentified to our knowledge. (C) Selective ion chromatograms (XICs) of ions with indicated m/z at specific liquid chromatography (LC) retention times corresponding to the elution times of the identified phosphopeptides in Table 1. XICs of Flag-Cav3.2 treated with or without calcineurin were compared. (D) A decrease in the phosphorylation of a diphosphorylated peptide was accompanied by an increase in the signal of its singly phosphorylated counterpart.

Preprints (www.preprints.org) | NOT PEER-REVIEWED | Posted: 16 August 2023 doi:10.20944/preprints202308.1114.v1



To validate the calcineurin-mediating dephosphorylation in culture cells, the Flag-Cav3.2 transfected HEK293 cells were treated with the calcineurin inhibitor cyclosporine A (CSA) for 24 hours. The XICs of S1198 and S2137 phosphorylated peptides showed increased ion intensities upon CSA treatment (Figure 2A). Furthermore, the phosphorylation signals of S1198 and S2137 in a calcineurin-binding deficient mutant of Cav3.2, the 9A-Cav3.2, were also increased compared to wild-type Cav3.2 (Figure 2B). These results suggest that calcineurin dephosphorylates Cav3.2 at S1198 and S2137 within HEK293 cells.

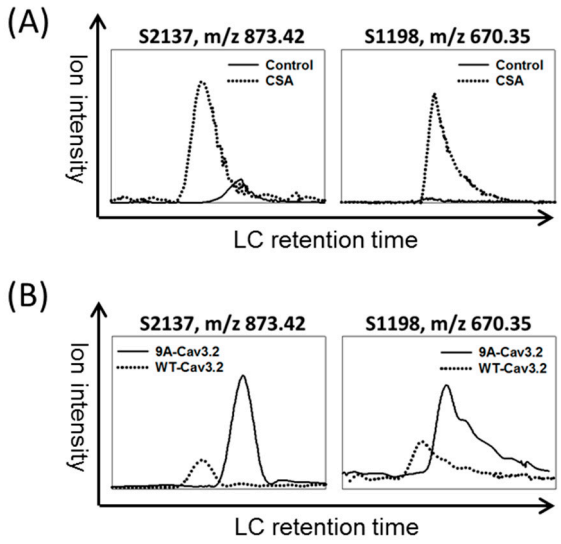


**Figure 2.** Regulation of Cav3.2 phosphorylation by calcineurin enzyme activity and binding Function in HEK293 cells. (A) Effect of calcineurin inhibition on Cav3.2 phosphorylation. HEK293 cells were transfected with Flag-Cav3.2 for 24 hours and then followed by a 24-hour inhibition of calcineurin using cyclosporine A (CSA). (B) Disruption of calcineurin binding function and Cav3.2 phosphorylation. HEK293 cells were transfected with Flag-tagged wildtype Cav3.2 or a calcineurin-binding deficient mutant, the 9A-Cav3.2, for 48 hours. XICs of peptides with indicated phosphorylation sites were compared.

### *3.2. CaMKII Kinase Phosphorylates S2137 of Cav3.2*

The potential kinases responsible for the identified phosphorylation sites in Cav3.2 were predicted based on kinase recognition motifs [28]. Table 2 reveals that 32 phosphorylation sites are associated with at least one potential kinase. Notably, the calcineurin-dephosphorylated sites S1198 and S2137 were both predicted to be substrates of CaMKII, PKD, or CHK1/2 kinases. Previous studies had revealed that S1198 of Cav3.2 can be phosphorylated by CaMKII [11,12]. Therefore, we sought to investigate whether S2137 is also a substrate of CaMKII. To explore this possibility, we incubated the GST-fusion C-terminus of Cav3.2 (GST-CII) with or without CaMKII. In CaMKII-treated samples, a subtle mobility shift of GST-CII bands was observed (Figure 3A). The SDS-PAGE gel bands containing GST-CII were subjected to trypsin digestion. The resulting tryptic peptides were then analyzed by LC-MS/MS and matched to the amino acid residues from 2135 to 2149 of human Cav3.2. We observed that the MSMS spectra of ions with m/z 873.40 corresponded to the S2137 phosphopeptide, while the MSMS spectra of ions with m/z 555.95 corresponded to the unphosphorylated peptide (Figure 3B). The S2137 phosphopeptide ion signal was exclusively found in the CaMKII-treated GST-CII, while the unphosphorylated peptide signal was almost absent. These results suggest that S2137 of full-length Cav3.2 can indeed be phosphorylated by CaMKII.

**Table 2.** Potential kinases targeting human Cav3.2 phosphorylation sites.

| Site | Domain | Predicted Kinase Motif[a] |
|---|---|---|
| S32 | N-terminal | CK1 (S-X-X-S/T) ERK (P-X-S/T-P, P-E-S/T-P) |

| | | |
|---|---|---|
| S44 | N-terminal | PKA (R-X-S/T) |
| S49 | N-terminal | CK2 (S/T-X-X-E) GSK3 (S-X-X-X-S) NEK6 (L-X-X-S/T) |
| S53 | N-terminal | CK1 (S/T-X-X-X-S) |
| S442 | I-II loop | CaMKII (R-X-X-S/T) AKT (R-X-R-X-X-S/T) |
| S558 | I-II loop | ERK (P-X-S/T-P) |
| S561 | I-II loop | CK1 (S-X-X-S/T) CDK2 (S/T-P-X-K/R) ERK (P-X-S/T-P) CDK1 (S/T-P-X-K/R) |
| S653 | I-II loop | CK1 (S-X-X-S/T) |
| S715 | I-II loop | CK2 (S/T-X-X-E) GSK3 (S-X-X-X-S) |
| S717 | I-II loop | NEK6 (L-X-X-S/T) |
| S719 | I-II loop | CK1 (S/T-X-X-X-S) |
| S722 | I-II loop | CK1 (S-X-X-S/T) |
| S758 | I-II loop | CDK2 (S/T-P-X-K/R) ERK (P-X-S/T-P) CDK1 (S/T-P-X-K/R) |
| S1035 | II-III loop | Aurora (R/K-X-S/T-I/L/V) |
| S1099 | II-III loop | GSK3 (S-X-X-X-S) |
| S1103 | II-III loop | CK1 (S/T-X-X-X-S) GSK3 (S-X-X-X-S) NEK6 (L-X-X-S/T) |
| S1107 | II-III loop | PKA (R-X-S/T, R-R/K-X-S/T) CK1 (S/T-X-X-X-S) CaMKII (R-X-X-S/T) AKT (R-R/S/T-X-S/T-X-S/T) |
| S1109 | II-III loop | CK1 (S-X-X-S/T) |
| S1144 | II-III loop | PKA (R-X-S/T, R-R/K-X-S/T) CK1 (S/T-X-X-X-S) CaMKII (R-X-X-S/T) AKT (R-R/S/T-X-S/T-X-S/T) |
| S1165 | II-III loop | PKA (R-X-S/T) Aurora (R/K-X-S/T-I/L/V) |
| S1168 | II-III loop | CK1 (S-X-X-S/T) |
| T1175 | II-III loop | CK2 (S/T-X-X-E) |
| S1198 | II-III loop | CaMKII (R-X-X-S/T) PKD (L/V/I-X-R/K-X-X-S/T) CHK1/2 (L-X-R-X-X-S/T) CHK1 (M/I/L/V-X-R/K-X-X-S/T) |
| S1587 | III-IV loop | PKA (R-X-S/T, R-R/K-X-S/T) GSK3 (S-X-X-X-S) CaMKII (R-X-X-S/T) |
| T1588 | III-IV loop | PKA (R-X-S/T, R-R/K-X-S/T) CaMKII (R-X-X-S/T) AKT (R-X-R-X-X-S/T) |
| S1591 | III-IV loop | CK1 (S/T-X-X-X-S) |
| S1604 | III-IV loop | CDK2 (S/T-P-X-K/R) CDK1 (S/T-P-X-K/R) |
| S1999 | C-terminal | CDK1 (S/T-P-K/R) |
| S2030 | C-terminal | CDK1 (S/T-P-K/R) |
| S2057 | C-terminal | CK1 (S-X-X-S/T) GSK3 (S-X-X-X-S) CDK2 (S/T-P-X-K/R) CDK1 (S/T-P-X-K/R) |
| S2137 | C-terminal | CaMKII (R-X-X-S/T, R-X-X-S/T-V) PKD (L/V/I-X-R/K-X-X-S/T) CHK1/2 (L-X-R-X-X-S/T) CHK1 (M/I/L/V-X-R/K-X-X-S/T) |
| S2222 | C-terminal | CaMKII (R-X-X-S/T) AKT (R-X-R-X-X-S/T) |

[a] Prediction was conducted using the entire amino acid sequence of human Cav3.2 through Phosida. .

To further investigate the phosphorylation regulation of Cav3.2 at S2137, we generated an antibody specifically targeting the phosphorylation at this site. To confirm the antibody's specificity for phospho-S2137, we expressed Flag-tagged wild-type, S1198A mutant, and S2137A mutant constructs of Cav3.2 into HEK293 cells. Compared with the untransfected control, the wild type and S1198A mutant generated signals of phospho-S2137 antibody. However, similar to the untransfected control, the S2137A mutant failed to generate signals using the phospho-S2137 antibody (Figure 3C). In alignment with the outcomes from our LC-MS/MS analysis, the phospho-S2137 antibody exhibited robust reactivity with the Flag-tagged full-length Cav3.2 following CaMKII treatment (Figure 3D). Furthermore, co-incubation with calcineurin led to the reduction of the phospho-S2137 antibody signal (Figure 3D). Our findings suggest that S2137 of full-length Cav3.2 undergoes phosphorylation by CaMKII and dephosphorylation by calcineurin.

Preprints (www.preprints.org) | NOT PEER-REVIEWED | Posted: 16 August 2023 doi:10.20944/preprints202308.1114.v1



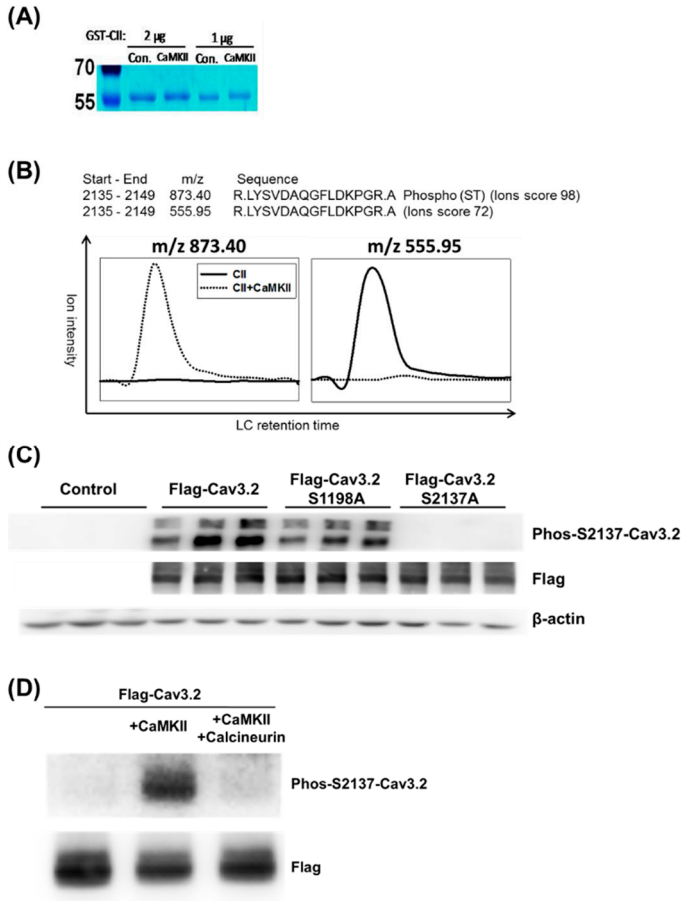


**Figure 3.** Identified S2137 as a novel CaMKII phosphorylation site on human Cav3.2. (A) CaMKII triggered a mobility shift in the SDS-PAGE gel for GST-CII, the GST-fusion protein derived from the C-terminus of Cav3.2. Incubation of GST-CII (1 or 2μg) with or without CaMKII was conducted. Molecular weight markers were designated in kD. (B) CaMKII increased the ion signal of phospho-S2137 peptide. Tryptic peptides extracted from GST-CII gel bands were analyzed by LC-MS/MS. An ion with m/z 873.40 was identified as the phospho-S2137 peptide, while another ion with m/z 555.95 corresponded to the unmodified peptide counterpart. (C) Verification of phospho-S2137 antibody specificity. The specificity of the antibody was confirmed by the signals generated from wild-type or mutant forms of Flag-tagged Cav3.2 expressed in HEK293 cells. (D) Cav3.2 S2137 phosphorylation by CaMKII and dephosphorylation by calcineurin in the full-length Cav3.2 were confirmed using phospho-S2137 antibody.

To investigate the native phosphorylation of S2137 of Cav3.2, we used mouse CAD cells, which express endogenous Cav3.2 [7,29]. The homolog sequences of human, rat, and mouse were aligned in the regions around human Cav3.2 S2137. In mice and rats, the homologous sites of human Cav3.2 S2137 are also serine residues and have CaMKII recognition motifs (Figure 4A). To detect the endogenous Cav3.2 S2137 phosphorylation, we employed the phospho-S2137 antibody. We used KCl-depolarization to increase the intracellular calcium concentration and CaMKII activity of mouse CAD cells [7,30]. A basal phospho-S2137 Cav3.2 signal in control CAD cells was detected by the antibody. When CAD cells were depolarized by KCl, the phosphorylation of Cav3.2 S2137 increased (Figure 4B). Our results suggest that there is endogenous phosphorylation of Cav3.2 S2137, and membrane depolarization of neuronal cell line enhances the phosphorylation of Cav3.2 S2137.

Preprints (www.preprints.org) | NOT PEER-REVIEWED | Posted: 16 August 2023 doi:10.20944/preprints202308.1114.v1



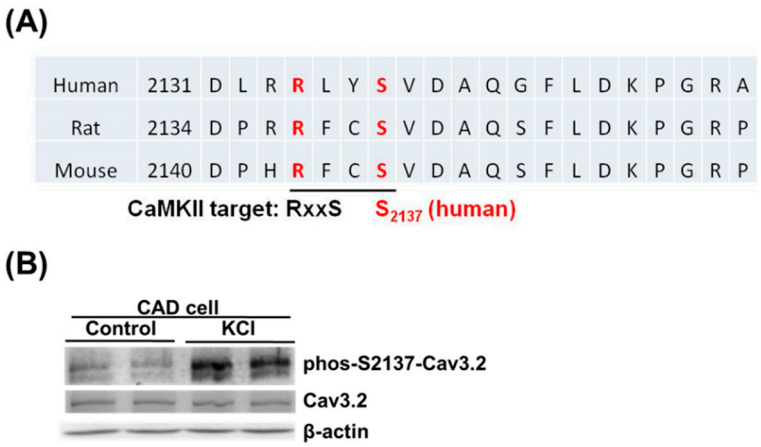


**Figure 4.** Phosphorylation of S2137 in endogenous Cav3.2 induced by membrane depolarization through KCl stimulation. (A) Alignment of Cav3.2 sequences from human, rat, and mouse around human Cav3.2 S2137. (B) KCl-induced membrane depolarization led to phosphorylation of S2137 in native Cav3.2 of mouse CAD cells. Cells were stimulated with 50 mM KCl for 5 minutes.

*3.3. Effect of S2137 Phosphorylation on Functional Properties of Cav3.2*

To investigate the impact of Cav3.2 S2137 phosphorylation on the calcium current properties of Cav3.2, we expressed the S2137D phosphorylation mimic mutant in HEK293 cells. The voltage-gated channel properties of wild-type and S2137D Cav3.2 were compared using a whole-cell voltage clamp. Transfected cells were held at -90 mV and then subjected to test potentials. The current densities of S2137D Cav3.2 were significantly smaller than those of wild-type Cav3.2 (Figure 5A).

Calcineurin binds to Cav3.2 and also dephosphorylates Cav3.2. To distinguish between the effects of calcineurin binding and dephosphorylation, we introduced the phospho-deficient S1198A and S2137A mutants into the calcineurin-binding-deficient 9A mutant of Cav3.2. In the 9A mutant, single mutations in S1198A or S2137A led to increased current densities of Cav3.2, but these changes did not reach statistical significance. However, when both sites were mutated to S1198AS2137A, the current density was significantly increased (Figure 5B). Our results suggest that phosphorylation of S2137 of Cav3.2 inhibits the current densities of Cav3.2 calcium channels, and dephosphorylation of Cav3.2 by calcineurin enhances the current densities of Cav3.2 calcium channels.

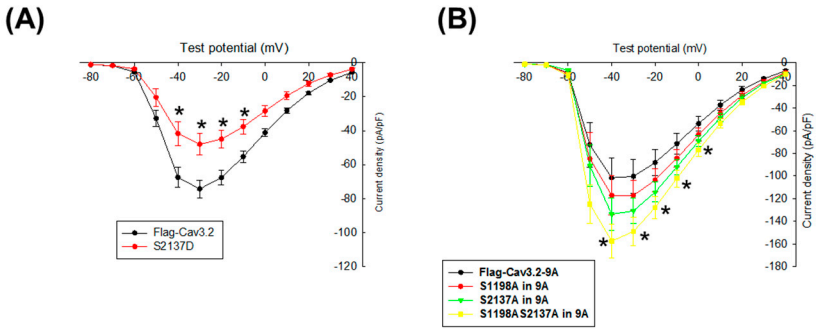


**Figure 5.** Mutation of S2137 modulated the Cav3.2 calcium channel function. (A) Phosphorylation mimic of S2137 inhibits Cav3.2 calcium current. To mimic phosphorylation, S2137 of Cav3.2 was mutated to aspartic acid, denoted as S2137D. Whole-cell voltage clamp was performed on HEK293 cells expressing either wild type (n=25) or S2137D (n=13) Cav3.2. The current density-voltage plots are presented. * P<0.05 compared to Flag-Cav3.2. (B) Phosphorylation of S1198 and S2137 directly impacted Cav3.2 calcium current. Whole-cell voltage clamp was performed on HEK293 cells expressing 9A-mutant (n=14) or S1198A in 9A (n=12) or S2137A in 9A (n=18) or S1198AS2137A in 9A (n=13). * P<0.05 compared to Flag-Cav3.2-9A.

 doi:10.20944/preprints202308.1114.v1



## 4. Discussion

Previously, the phosphorylation of Cav3.2 by various kinases has been elucidated [9]. In this study, we identified dephosphorylation sites on Cav3.2 by calcineurin, both in vitro and in vivo. We discovered that calcineurin dephosphorylates the previously identified CaMKII target site, S1198, on Cav3.2. Additionally, we revealed that a novel CaMKII target site, S2137, on Cav3.2 is also subjected to dephosphorylation by calcineurin. To specifically recognize phospho-S2137 Cav3.2, we generated an antibody, and with its application, we confirmed that membrane depolarization increases the phosphorylation of Cav3.2 at S2137. Lastly, we observed that S2137 phosphorylation modulates the calcium channel function of Cav3.2.

In this study, our findings indicate that the residues in the C-terminus of Cav3.2 undergo more significant dephosphorylation by calcineurin when compared to the residues in the II-III loop. The docking of calcineurin to its substrates is a crucial step in the dephosphorylation of various calcineurin targets [31]. Moreover, the specificity of calcineurin-mediated dephosphorylation relies more on the structural characteristics of substrates rather than a specific consensus sequence [32]. Notably, our findings demonstrate that the sites on Cav3.2 dephosphorylated by calcineurin lack a distinct sequence pattern. Since the substrate-binding site is located within the catalytic domain of calcineurin, a higher degree of dephosphorylation is expected in the C-terminus of Cav3.2, as observed in our study. Interestingly, the phosphorylation level of Cav3.2 at S2188, which is situated close to the PCISVE (2190-2195) calcineurin binding motif of Cav3.2, was found to be augmented by the addition of calcineurin. This observation raises the possibility that the protein/protein binding region might create an environment conducive to stabilizing the phosphorylated motifs.

Previously, CaMKII had been identified as the enzyme phosphorylating S1198 of Cav3.2, a process that facilitates the opening of channels near the membrane potential [11,12]. However, in the current study, we uncovered that S1198 of Cav3.2 can also be targeted for dephosphorylation by calcineurin. Moreover, our investigation revealed a previously unknown phosphorylation target of CaMKII, S2137 of Cav3.2, which interestingly is also subject to dephosphorylation by calcineurin. Notably, when analyzing CAD cells that naturally express Cav3.2, we detected an increased signal of phospho-S2137 Cav3.2 antibody after membrane depolarization caused by KCl. Given that membrane depolarization prompts the opening of Cav3.2, our findings suggest that calcium influx through these channels might stimulate the phosphorylation of Cav3.2 by CaMKII, rather than inducing dephosphorylation by calcineurin. In earlier investigations, we observed a peak binding of calcineurin with Cav3.2 at a calcium concentration of 30 μM, along with 20% binding at a calcium concentration of 1 μM [17]. Given the usual cytoplasmic calcium concentration span of 0.1 μM in resting cells to 1 μM in depolarized cells [33], it becomes plausible that the activation of calcineurin could take place in scenarios where there is an excessive influx of calcium through Cav3.2. Moreover, given that CaMKII binds to the II-III loop where S1198 is located, and calcineurin binds to the C-terminus where S2137 is situated, it is plausible that CaMKII would have a preference for phosphorylating S1198 over S2137, while calcineurin could have a predilection for dephosphorylating S2137 rather than S1198. These spatial arrangements of upstream regulators and downstream target sites contribute to the nuanced fine-tuning of the Cav3.2 channel function.

Owing to advancements in mass spectrometry technology, the identification of phosphorylation sites in proteins of interest is now a commonly conducted practice [34]. Previously, Blesneac et al. identified 34 distinct phosphorylation sites from rat brains and 43 phosphorylation sites from human Cav3.2 overexpressed in HEK293T cells using mass spectrometry technology [26]. In this study, we identified 36 phosphorylation sites in human Cav3.2, and among them, 8 phosphorylation sites are novel to our knowledge. The potential implications of these Cav3.2 phosphorylation sites can be speculated by comparing them with variant sequences of Cav3.2 from humans with phenotypes in the ClinVar database [35]. In addition to identification, our study expands the scope by incorporating phosphopeptide quantification, allowing us to uncover novel target sites of calcineurin and CaMKII. Furthermore, this phosphopeptide quantification strategy revealed varying fold changes among the target sites, indicating differences in the prioritization of phosphorylation or dephosphorylation among these targets.

Certain clinical agents are categorized as T-type calcium channel blockers and are used for treating epilepsy and hypertension [36]. Moreover, T-type calcium channel blockers exhibit promising potential for pain management as well [37]. Given that there are three subtypes of T-type calcium channels in humans, namely Cav3.1, Cav3.2, and Cav3.3, the development of subtype-specific inhibitors for these channels is considered essential for both therapeutic and research purposes [38]. Research has shown that intrathecal administration of the deubiquitination target peptide of Cav3.2 to mice resulted in an analgesic effect in the context of neuropathic and inflammatory pain [7]. Cell-permeable phosphopeptides have been employed to either inhibit or stimulate intracellular signaling pathways [39]. We are confident that identifying Cav3.2 phosphopeptides regulated by kinases or phosphatases will advance our comprehension of channel regulation and consequently contribute to the development of treatment strategies.

## 5. Conclusions

The current study has unveiled the sites on Cav3.2 channels that undergo dephosphorylation by calcineurin. Among these calcineurin-dephosphorylated residues, S1198, situated in the II-III loop of Cav3.2, had been previously identified as a target site for CaMKII phosphorylation. Additionally, we have identified a novel site, S2137, located in the C-terminus of Cav3.2, which is both phosphorylated by CaMKII and dephosphorylated by calcineurin. Notably, membrane depolarization in mouse CAD cells led to the phosphorylation of S2137, a phenomenon confirmed by the specific antibody designed for this purpose. Furthermore, our study delved into the functional implications associated with S2137 phosphorylation.

**Supplementary Materials:** The following supporting information can be downloaded at: www.mdpi.com/xxx/s1, Figure S1: Approach for identifying calcineurin-dephosphorylated residues on Cav3.2 T-type calcium channel. ; Figure S2: Mascot search results of MSMS spectra.

**Author Contributions:** Conceptualization, C.-C.C. and Y.-W.C.; methodology, C.-C.C., Y.-C.C and Y.-W.C.; formal analysis, Y.-C.C and Y.-W.C.; resources, C.-C.C.; writing—original draft preparation, Y.-C.C and Y.-W.C.; writing—review and editing, C.-C.C. and Y.-W.C.; supervision, C.-C.C.; project administration, C.-C.C.; funding acquisition, C.-C.C. All authors have read and agreed to the published version of the manuscript.

**Funding:** This work was supported by Academia Sinica (AS-IR-112-05-A) to CC Chen.

**Institutional Review Board Statement:** Not applicable.

**Informed Consent Statement:** Not applicable.

**Data Availability Statement:** Not applicable.

**Acknowledgments:** We thank Geen-Dong Chang from National Taiwan University for providing valuable assistance in antibody generation. We thank Yu-Ju Chen from the Institute of Chemistry, Academia Sinica for the help in mass spectrometry analysis. We thank the mass spectrometry center of the Institute of Chemistry, and the Common Equipment Core at the Institute of Biomedical Sciences, Academia Sinica, Taiwan.

**Conflicts of Interest:** The authors declare no conflict of interest. The funders had no role in the design of the study; in the collection, analyses, or interpretation of data; in the writing of the manuscript, or in the decision to publish the results.

## References

1. Catterall, W.A. Voltage-Gated Calcium Channels. *Csh Perspect Biol* **2011**, *3*, a003947.
2. Missiaen, L.; Callewaert, G.; Parys, J.B.; Wuytack, F.; Raeymaekers, L.; Droogmans, G.; Nilius, B.; Eggermont, J.; De Smedt, H. [Intracellular calcium: physiology and physiopathology]. *Verh K Acad Geneeskd Belg* **2000**, *62*, 471-499.
3. Catterall, W.A.; Lenaeus, M.J.; El-Din, T.M.G. Structure and Pharmacology of Voltage-Gated Sodium and Calcium Channels. *Annu Rev Pharmacol* **2020**, *60*, 133-154.
4. Melgari, D.; Frosio, A.; Calamaio, S.; Marzi, G.A.; Pappone, C.; Rivolta, I. T-Type Calcium Channels: A Mixed Blessing. *Int J Mol Sci* **2022**, *23*, 9894.
5. Weiss, N.; Zamponi, G.W. Genetic T-type calcium channelopathies. *J Med Genet* **2020**, *57*, 1-10.

6. Bourinet, E.; Alloui, A.; Monteil, A.; Barrere, C.; Couette, B.; Poirot, O.; Pages, A.; McRory, J.; Snutch, T.P.; Eschalier, A., et al. Silencing of the Ca(v)3.2 T-type calcium channel gene in sensory neurons demonstrates its major role in nociception. *Embo J* **2005**, *24*, 315-324.
7. Garcia-Caballero, A.; Gadotti, V.M.; Stemkowski, P.; Weiss, N.; Souza, I.A.; Hodgkinson, V.; Bladen, C.; Chen, L.; Hamid, J.; Pizzoccaro, A., et al. The deubiquitinating enzyme USP5 modulates neuropathic and inflammatory pain by enhancing Cav3.2 channel activity. *Neuron* **2014**, *83*, 1144-1158.
8. Huang, J.T.; Zamponi, G.W. Regulation of voltage gated calcium channels by GPCRs and post-translational modification. *Curr Opin Pharmacol* **2017**, *32*, 1-8.
9. Sharma, A.; Rahman, G.; Gorelik, J.; Bhargava, A. Voltage-Gated T-Type Calcium Channel Modulation by Kinases and Phosphatases: The Old Ones, the New Ones, and the Missing Ones. *Cells-Basel* **2023**, *12*, 461.
10. Hu, C.; Depuy, S.D.; Yao, J.; McIntire, W.E.; Barrett, P.Q. Protein kinase A activity controls the regulation of T-type CaV3.2 channels by Gbetagamma dimers. *J Biol Chem* **2009**, *284*, 7465-7473.
11. Yao, J.; Davies, L.A.; Howard, J.D.; Adney, S.K.; Welsby, P.J.; Howell, N.; Carey, R.M.; Colbran, R.J.; Barrett, P.Q. Molecular basis for the modulation of native T-type Ca2+ channels in vivo by Ca2+/calmodulin-dependent protein kinase II. *J Clin Invest* **2006**, *116*, 2403-2412.
12. Welsby, P.J.; Wang, H.; Wolfe, J.T.; Colbran, R.J.; Johnson, M.L.; Barrett, P.Q. A mechanism for the direct regulation of T-type calcium channels by Ca2+/calmodulin-dependent kinase II. *J Neurosci* **2003**, *23*, 10116-10121.
13. Gomez, K.; Calderon-Rivera, A.; Sandoval, A.; Gonzalez-Ramirez, R.; Vargas-Parada, A.; Ojeda-Alonso, J.; Granados-Soto, V.; Delgado-Lezama, R.; Felix, R. Cdk5-Dependent Phosphorylation of Ca(v)3.2 T-Type Channels: Possible Role in Nerve Ligation-Induced Neuropathic Allodynia and the Compound Action Potential in Primary Afferent C Fibers. *Journal of Neuroscience* **2020**, *40*, 283-296.
14. Iftinca, M.; Hamid, J.; Chen, L.; Varela, D.; Tadayonnejad, R.; Altier, C.; Turner, R.W.; Zamponi, G.W. Regulation of T-type calcium channels by Rho-associated kinase. *Nat Neurosci* **2007**, *10*, 854-860.
15. Park, J.Y.; Jeong, S.W.; Perez-Reyes, E.; Lee, J.H. Modulation of Ca(v)3.2 T-type Ca2+ channels by protein kinase C. *Febs Lett* **2003**, *547*, 37-42.
16. Weiss, N.; Hameed, S.; Fernandez-Fernandez, J.M.; Fablet, K.; Karmazinova, M.; Poillot, C.; Proft, J.; Chen, L.N.; Bidaud, I.; Monteil, A., et al. A Ca(v)3.2/Syntaxin-1A Signaling Complex Controls T-type Channel Activity and Low-threshold Exocytosis. *Journal of Biological Chemistry* **2012**, *287*, 2810-2818.
17. Huang, C.H.; Chen, Y.C.; Chen, C.C. Physical interaction between calcineurin and Cav3.2 T-type Ca2+ channel modulates their functions. *Febs Lett* **2013**, *587*, 1723-1730.
18. Chen, L.; Song, M.; Yao, C.Y. Calcineurin in development and disease. *Genes Dis* **2022**, *9*, 915-927.
19. Molkentin, J.D.; Lu, J.R.; Antos, C.L.; Markham, B.; Richardson, J.; Robbins, J.; Grant, S.R.; Olson, E.N. A calcineurin-dependent transcriptional pathway for cardiac hypertrophy. *Cell* **1998**, *93*, 215-228.
20. Wilkins, B.J.; Dai, Y.S.; Bueno, O.F.; Parsons, S.A.; Xu, J.; Plank, D.M.; Jones, F.; Kimball, T.R.; Molkentin, J.D. Calcineurin/NFAT coupling participates in pathological, but not physiological, cardiac hypertrophy. *Circ Res* **2004**, *94*, 110-118.
21. Chiang, C.S.; Huang, C.H.; Chieng, H.L.; Chang, Y.T.; Chang, D.R.; Chen, J.J.; Chen, Y.C.; Chen, Y.H.; Shin, H.S.; Campbell, K.P., et al. The Ca(v)3.2 T-Type Ca2+ Channel Is Required for Pressure Overload-Induced Cardiac Hypertrophy in Mice. *Circulation Research* **2009**, *104*, 522-530.
22. Han, C.L.; Chien, C.W.; Chen, W.C.; Chen, Y.R.; Wu, C.P.; Li, H.; Chen, Y.J. A Multiplexed Quantitative Strategy for Membrane Proteomics OPPORTUNITIES FOR MINING THERAPEUTIC TARGETS FOR AUTOSOMAL DOMINANT POLYCYSTIC KIDNEY DISEASE. *Mol Cell Proteomics* **2008**, *7*, 1983-1997.
23. Chang, Y.W.; Chang, Y.T.; Wang, Q.C.; Lin, J.J.C.; Chen, Y.J.; Chen, C.C. Quantitative Phosphoproteomic Study of Pressure-Overloaded Mouse Heart Reveals Dynamin-Related Protein 1 as a Modulator of Cardiac Hypertrophy. *Mol Cell Proteomics* **2013**, *12*, 3094-3107.
24. Savitski, M.M.; Lemeer, S.; Boesche, M.; Lang, M.; Mathieson, T.; Bantscheff, M.; Kuster, B. Confident Phosphorylation Site Localization Using the Mascot Delta Score. *Mol Cell Proteomics* **2011**, *10*, doi:ARTN M110.003830.
25. Tsou, C.C.; Tsai, C.F.; Tsui, Y.H.; Sudhir, P.R.; Wang, Y.T.; Chen, Y.J.; Chen, J.Y.; Sung, T.Y.; Hsu, W.L. IDEAL-Q, an Automated Tool for Label-free Quantitation Analysis Using an Efficient Peptide Alignment Approach and Spectral Data Validation. *Mol Cell Proteomics* **2010**, *9*, 131-144.
26. Blesneac, I.; Chemin, J.; Bidaud, I.; Huc-Brandt, S.; Vandermoere, F.; Lory, P. Phosphorylation of the Cav3.2 T-type calcium channel directly regulates its gating properties. *P Natl Acad Sci USA* **2015**, *112*, 13705-13710.
27. Hornbeck, P.V.; Zhang, B.; Murray, B.; Kornhauser, J.M.; Latham, V.; Skrzypek, E. PhosphoSitePlus, 2014: mutations, PTMs and recalibrations. *Nucleic Acids Res* **2015**, *43*, D512-D520.
28. Gnad, F.; Gunawardena, J.; Mann, M. PHOSIDA 2011: the posttranslational modification database. *Nucleic Acids Res* **2011**, *39*, D253-260.
29. Garcia-Caballero, A.; Gandini, M.A.; Huang, S.; Chen, L.; Souza, I.A.; Dang, Y.L.; Stutts, M.J.; Zamponi, G.W. Cav3.2 calcium channel interactions with the epithelial sodium channel ENaC. *Mol Brain* **2019**, *12*, 12.

30. Bok, J.; Wang, Q.; Huang, H.; Green, S.H. CaMKII and CaMKIV mediate distinct prosurvival signaling pathways in response to depolarization in neurons. *Mol Cell Neurosci* **2007**, *36*, 13-26.
31. Li, H.M.; Rao, A.; Hogan, P.G. Interaction of calcineurin with substrates and targeting proteins. *Trends Cell Biol* **2011**, *21*, 91-103.
32. Donelladeana, A.; Krinks, M.H.; Ruzzene, M.; Klee, C.; Pinna, L.A. Dephosphorylation of Phosphopeptides by Calcineurin (Protein Phosphatase 2b). *Eur J Biochem* **1994**, *219*, 109-117.
33. Bagur, R.; Hajnoczky, G. Intracellular Ca2+ Sensing: Its Role in Calcium Homeostasis and Signaling. *Mol Cell* **2017**, *66*, 780-788.
34. Dephoure, N.; Gould, K.L.; Gygi, S.P.; Kellogg, D.R. Mapping and analysis of phosphorylation sites: a quick guide for cell biologists. *Mol Biol Cell* **2013**, *24*, 535-542.
35. Landrum, M.J.; Lee, J.M.; Riley, G.R.; Jang, W.; Rubinstein, W.S.; Church, D.M.; Maglott, D.R. ClinVar: public archive of relationships among sequence variation and human phenotype. *Nucleic Acids Res* **2014**, *42*, D980-D985.
36. Kopecky, B.J.; Liang, R.Q.; Bao, J.X. T-type calcium channel blockers as neuroprotective agents. *Pflug Arch Eur J Phy* **2014**, *466*, 757-765.
37. Harding, E.K.; Zamponi, G.W. Central and peripheral contributions of T-type calcium channels in pain. *Molecular Brain* **2022**, *15*, 39.
38. Herzig, V.; Chen, Y.C.; Chin, Y.K.; Dekan, Z.; Chang, Y.W.; Yu, H.M.; Alewood, P.F.; Chen, C.C.; King, G.F. The Tarantula Toxin omega-Avsp1a Specifically Inhibits Human Ca(V)3.1 and Ca(V)3.3 via the Extracellular S3-S4 Loop of the Domain 1 Voltage-Sensor. *Biomedicines* **2022**, *10*, 1066.
39. Dunican, D.J.; Doherty, P. Designing cell-permeant phosphopeptides to modulate intracellular signaling pathways. *Biopolymers* **2001**, *60*, 45-60.